DOI: 10.37943/23KFOU5095

Nurassyl Zhomartkan

Bachelor of science, Junior researcher, Laboratory of Digital Technologies and Modeling zhomartkan.kz@mail.ru, orcid.org/0009-0006-3935-2013 Sarsen Amanzholov East Kazakhstan University, Kazakhstan

Anatoliy Pavlenko

Master of Natural Sciences, Senior Lecturer, Higher school of IT and natural sciences ellezard@mail.ru, orcid.org/0000-0001-8556-6633 Sarsen Amanzholov East Kazakhstan University, Kazakhstan

Yerzhan Baiburin

Senior researcher, Laboratory of Digital Technologies and Modeling ebaiburin@vku.edu.kz, orcid.org/0000-0002-1583-9912 Sarsen Amanzholov East Kazakhstan University, Kazakhstan

Mohammad Alhuyi-Nazari

PhD in Energy System Engineering, School of Energy Engineering and Sustainable Resources, College of Interdisciplinary Science and Technology

nazari.mohammad.a@ut.ac.ir, orcid.org/0000-0001-8223-7519 University of Tehran, Iran

MODELING AND WEB-BASED VISUALIZATION OF FLOOD ZONES: A CASE STUDY OF THE BUKTYRMA RIVER SECTION

Abstract: This study focuses on flood risk assessment in a vulnerable reach of the Buktyrma River basin, located in the East Kazakhstan region. The main goal was to develop and validate a modelling workflow that uses open-access data and software to simulate flood dynamics and visualize the results through an interactive GIS-based interface. The approach involved statistical analysis of 24 years of annual maximum discharge and water level data from gauging station to define a representative flood event. Terrain data were derived from the 30 m Copernicus Digital Elevation Model, which was used to construct the hydraulic geometry of the study area. Two-dimensional flood modeling was carried out in HEC-RAS 6.6, incorporating spatially differentiated Manning's roughness values based on cadastral land-use classification maps.

The modeling results were verified using satellite imagery from Landsat 7 by calculating the Normalized Difference Water Index for the 2018 flood event, which had a 4% exceedance probability. The comparison showed a high degree of agreement, indicating that the simulated flood zone overlapped 87% with the NDWI-derived water mask, and the total inundation area differed by less than 2%. Model outputs such as flood depth, flow velocity, and cross-sectional profiles were visualized, and the resulting flood map was uploaded within a web-GIS platform. The study demonstrates a transparent and cost-effective methodology that can be applied to other river basins in Kazakhstan, offering a practical tool for spatial planning, risk mitigation, and early warning systems based entirely on publicly available data and software.

Keywords: flood modelling; HEC-RAS; web-GIS; NDWI; Landsat-7; Copernicus DEM; Buktyrma River

Copyright © 2025, Authors. This is an open access article under the Creative Commons CC BY-NC-ND license Received: 29.08.2025 Accepted: 24.09.2025 Published: 30.09.2025

Introduction

Flooding is considered one of the most devastating natural disasters. It poses a threat to the life and health of the population, infrastructure, economy and the environment. Studies show that about 350 million people worldwide are affected by floods [1]. Despite this, many cities around the world remain insufficiently prepared for its severe consequences [2].

According to the Emergency Committee of the Ministry of Internal Affairs of the Republic of Kazakhstan, approximately 48 201 km² of territory is at risk of flooding because of spring floods [3]. However, the population is poorly informed about the rules of conduct in emergency situations and is not engaged in self-protection measures [4]. The East Kazakhstan Region is especially at risk, as it holds over 40% of national water resources and five hydroelectric power plants. As a result, flooding emergencies are recorded annually. Many villages, residential houses, social and transport infrastructure facilities, as well as agricultural lands, farms, pastures, and livestock are located within the flood zone.

The use of information and communication technologies (ICT) in the field of hydrodynamic modeling makes it possible to predict the spatial and temporal distribution of flood waters, assess risks, and form data-based mitigation solutions [4], [5]. One-dimensional (1D) modeling assumes the movement of water only along the main channel. It is suitable for representing processes in a river; however, when calculating water beyond the channel and its spread over the floodplain, two-dimensional (2D) modeling gives more accurate results [3], [6]. 2D accounts for both longitudinal and transverse flow, while three-dimensional (3D) adds a vertical component. The use of a digital elevation model (DEM) with high spatial resolution can significantly improve the accuracy of flood modeling and reduce the level of uncertainty [7]. A DEM is a topographic representation of the earth's surface without considering vegetation, buildings, or other objects. The grid format of DEM is the most widely used in hydrological modeling, as it provides a convenient data structure for spatial analysis and integration with GIS and hydrodynamic models.

The MIKE 21 and HEC-RAS software packages are widely used to perform hydraulic calculations [3]. MIKE 21 allows additional physical processes to be considered, which can make the simulation more realistic, but the program is more complicated and requires more time for post-processing [8]. HEC-RAS, on the other hand, has high accuracy, a user-friendly interface, and the ability to integrate with geographic information systems (GIS) for spatial analysis of flood sites [6] and preliminary identification of flood-prone sites [10]. The key parameters used in HEC-RAS when constructing the model are the geometric characteristics of the channel: centerlines, banks, flow paths, and cross-sections [9]. Since version 5.0, HEC-RAS has included a 2D module that allows for estimating the distribution of water over an area with high accuracy [10], comparable to several commercial hydrodynamic models. Thus, HEC-RAS 2D was compared with IBER 2D, and the results showed that both models provide accurate forecasts of water depth and flood area [6]. Research shows that HEC-RAS demonstrates high accuracy and efficiency compared to other models such as TUFLOW, MIKE FLOOD, and SOBEK [11].

Kazakhstani scientists successfully use the HEC-RAS model to assess flood hazards in the Zhabay River basin (accuracy 81–86%) [12], to simulate the operation of sluices in the irrigation system between the Nura and Yesil rivers (accuracy 70%) [13], and to create flood hazard maps for the Yesil River (accuracy 59.7%) [11].

However, HEC-RAS has its limitations, including insufficient detail in representing complex geometries and boundary conditions, as well as significant computational costs when modeling large-scale hydrodynamic processes [14]. The full dynamic mode in HEC-RAS can sometimes lead to overestimation of flood zones [15]. For producing flood maps of entire river

networks at regional or continental scales, models such as LISFLOOD-FP and AutoRAPID are more appropriate [16].

The analysis of hydrological data for the East Kazakhstan Region showed their insufficient completeness and continuity [17]. Of the 48 operating hydrological posts in the state network, only 26 have continuous observation series lasting more than 10 years, which significantly limits the possibilities of integrated modeling at the regional level. In such circumstances, the most reasonable approach is to conduct initial studies at individual sites. This will allow researchers to develop techniques and approaches on local cases, with subsequent scaling as data availability expands.

Given the high frequency of floods in the East Kazakhstan Region and the significant vulnerability of residential and critical infrastructure, it is becoming especially important to introduce digital tools for monitoring, modeling, and visualizing hydrological risks. Modern ICT tools, including GIS and hydrodynamic modeling, not only provide a visual representation of hazardous areas, but also create the basis for automated assessment of emergency scenarios. The development of integrated ICT solutions in this area is relevant in terms of increasing the resilience of territories to hydrometeorological threats and supporting operational management decision-making.

The aim of this study is to test an approach to digital modeling and visualization of flood scenarios using the HEC-RAS hydrodynamic model. The research objectives are as follows:

To analyze available hydrological data.

To prepare an open Copernicus DEM and perform spatial classification of land-use zones.

To develop and calibrate a hydraulic flood model in HEC-RAS based on scenarios of varying intensity.

To integrate the modeling results into a GIS platform for interactive flood visualization.

Methods and Materials

Study area

A reach of the Buktyrma River near Lesnaya Pristan (Altai District, East Kazakhstan Region; 49.8960° N, 84.3293° E) was selected for hydraulic modeling. The selection was based on frequent flood occurrences during spring snowmelt and autumn rain-on-snow events, and the availability of long-term stage-discharge data from gauging post No. 11129 for model calibration.

The Buktyrma is a mountain river with mixed feeding, formed mainly by snowmelt and rainfall. The highest discharges and water levels are recorded during the spring flood period (late April to early June). However, when intensive rainfall coincides with elevated temperatures, secondary floods are possible in August–November, during which water levels may reach values comparable to the spring maximum. The landscapes of the valley are characterized by an asymmetric structure: a distinct floodplain, one or two floodplain terraces, and the surrounding slope systems. The channel flows in a meandering course within the floodplain, whose width varies from 200 to 450 m. The slopes are covered with mixed coniferous–broadleaf forests, alternating in places with open steppe areas and agricultural lands. These morphological and phytogeographic features increase the heterogeneity of the stream's hydraulic parameters and, consequently, the complexity of accurately predicting flood zones.

Hydrological data

To define a representative flood scenario for modeling, annual maximum discharge and water level records from Kazhydromet were analysed for gauging station N^2 11129 for the period 1998–2021. To determine the threshold at which flooding occurs, exceedance probabilities were calculated using a ranked-series approach based on the Kritsky–Menkel equation (Equation 1), which provides an unbiased empirical estimate suitable for limited datasets.

$$p_m = \frac{m}{n+1} 100\%,\tag{1}$$

where p_m the empirical exceedance probability (in %), m is the rank of the observation in the ordered series (starting from the largest value), and n is the total number of observations [18].

Smoothing the results of empirical data and forecasting rare floods are carried out using analytical curves. In this work, an analytical curve based on the continuous Pearson Type III distribution is used, whose probability density functions satisfy the differential equation:

$$\frac{dy}{dz} = \frac{y(z+a)}{b_0 + b_1 z},\tag{2}$$

where z is a random variable associated with the initial random variable X by the relation

$$z = k - 1, (3)$$

where k is the modular coefficient; y is the ordinate of the probability density function of the random variable Z; a is the distance from the center of the distribution (mk) to the mode (M_0) ; b_0 and b_1 are parameters (real numbers) that can be varied to obtain different types of distribution curves.

In practice, the random variable X is often replaced with modular coefficients (k_i) , and the random variable X is substituted with a standardized (normalized) random variable (t_i) .

The standard normalized variable can be obtained from the series X using the formula 4.

$$t_i = \frac{x_i - m_x}{s_x},\tag{4}$$

where t_i is the normalized ordinate for the value x_i , x_i is the specific value of water level or discharge, m_x is the mean of the series, s_x is the standard deviation of the series.

The highest recorded flood had a discharge of 2140 m³/s and a stage of 710 cm, corresponding to a 4% exceedance probability (Table 1). This event was selected as the design flood scenario for hydraulic modeling and GIS-based visualization.

Table 1. Annual maximum discharge and water level values for the Buktyrma River (1998–2021), ranked series and calculated exceedance probabilities.

mi	Annual maximum discharge (m³/s)	Annual maximum water level (cm)	Ranked discharge (m³/s)	Ranked water level (cm)	Exceedance probability (%)
1	1260	531	2140	710	4
2	989	483	1910	666	8
3	1070	494	1580	590	12
4	1910	590	1490	552	16
5	1460	520	1460	536	20
6	1190	472	1440	531	24
7	1210	515	1440	530	28
8	1110	498	1430	526	32
9	1310	530	1340	520	36
10	1240	518	1310	518	40
11	908	460	1260	515	44
12	1200	498	1240	512	48
13	1440	536	1230	508	52
14	1060	467	1210	508	56
15	595	377	1200	498	60

© Nurassyl Zhomartkan, Anatoliy Pavlenko, Yerzhan Baiburin, Mohammad Alhuyi-Nazari

16	1340	512	1190	498	64
17	1580	552	1160	494	68
18	2140	666	1110	487	72
19	1430	526	1070	483	76
20	1230	508	1060	481	80
21	1160	710	1060	472	84
22	1440	487	989	467	88
23	1490	508	908	460	92
24	1060	481	595	377	96

Topographic and land-cover data

As the topographic basis, the Copernicus DEM with a resolution of 30×30 m was used. The dataset (ID: OTSDEM.032021.4326.3), obtained from OpenTopography, is based on radar stereoscopy (TanDEM-X/WorldDEM, 2011-2015) and provided by the European Space Agency for scientific use [19]. The DEM covers the river channel and adjacent areas, including the floodplain, terraces, and surrounding slopes.

To support spatial differentiation of surface types, land-use data were extracted from the Public Cadastral Map of the Republic of Kazakhstan, accessed via the Unified State Cadastral System [20]. Four general land-use categories were identified:

- agricultural lands (arable fields, hayfields, and pastures);
- special-purpose territories (mining sites, quarries, and artificial reservoirs);
- anthropogenically transformed zones (settlements and industrial sites);
- natural ecosystems (forests, shrub communities, and specially protected natural areas).

These cadastral data were reprojected to the WGS 84 / UTM Zone 45 N coordinate system and integrated into the modeling workflow for assigning spatially varying surface roughness. Hydraulic modeling in HEC-RAS

The 30 m DEM was imported into HEC-RAS 6.6, where it was clipped to the study area and used to generate a 5 m-resolution computational grid. This resampling allowed for detailed representation of the valley morphology, including microrelief features affecting flooding. HEC-RAS solves the two-dimensional Saint-Venant equations to model water surface dynamics and floodplain flow characteristics [21], [22]:

$$\frac{\partial \zeta}{\partial t} + \frac{\partial p}{\partial x} + \frac{\partial q}{\partial y} = 0, \tag{5}$$

$$\frac{\partial p}{\partial t} + \frac{\partial}{\partial x} \left(\frac{p^2}{h} \right) + \frac{\partial}{\partial y} \left(\frac{pq}{h} \right) = -\frac{n^2 p g \sqrt{p^2 + q^2}}{h^2} - g h \frac{\partial \zeta}{\partial x} + p f + \frac{\partial}{p \partial x} (h \tau_{xx}) + \frac{\partial}{p \partial y} (h \tau_{xx}), \tag{6}$$

$$\frac{\partial q}{\partial t} + \frac{\partial}{\partial y} \left(\frac{q^2}{h} \right) + \frac{\partial}{\partial x} \left(\frac{pq}{h} \right) = -\frac{n^2 pg \sqrt{p^2 + q^2}}{h^2} - gh \frac{\partial \zeta}{\partial y} + qf + \frac{\partial}{p\partial y} \left(h\tau_{yy} \right) + \frac{\partial}{p\partial x} \left(h\tau_{yy} \right), \tag{7}$$

where h is water depth (m), p and q are specific flow rates in the x and y directions (m³/s), ζ is surface (m), g is gravitational acceleration (m/s²), n is Manning coefficient, q is water density (kg/m³), $h\tau_{xx}$, $h\tau_{yy}$ are effective shear stress components, f is Coriolis force.

To improve the accuracy of modeling in HEC-RAS, Manning's roughness coefficients were assigned to each land-use category based on cadastral data, satellite imagery, and reference values from literature. Table 2 lists the values used in the model.

Land-cover type	Manning's n
Arable land	0.030
Hayfields / pastures	0.035
Sparse woodland	0.070
Dense forest	0.100
Residential areas	0.120
Roads, open spaces	0.020
Water surfaces	0.030
Industrial zones, quarries	0.040

Table 2. Manning's roughness coefficients (n) by land-cover type.

The application of the differentiation method significantly increased the accuracy of modeling by accounting for the spatial heterogeneity of the study area (Figure 1).

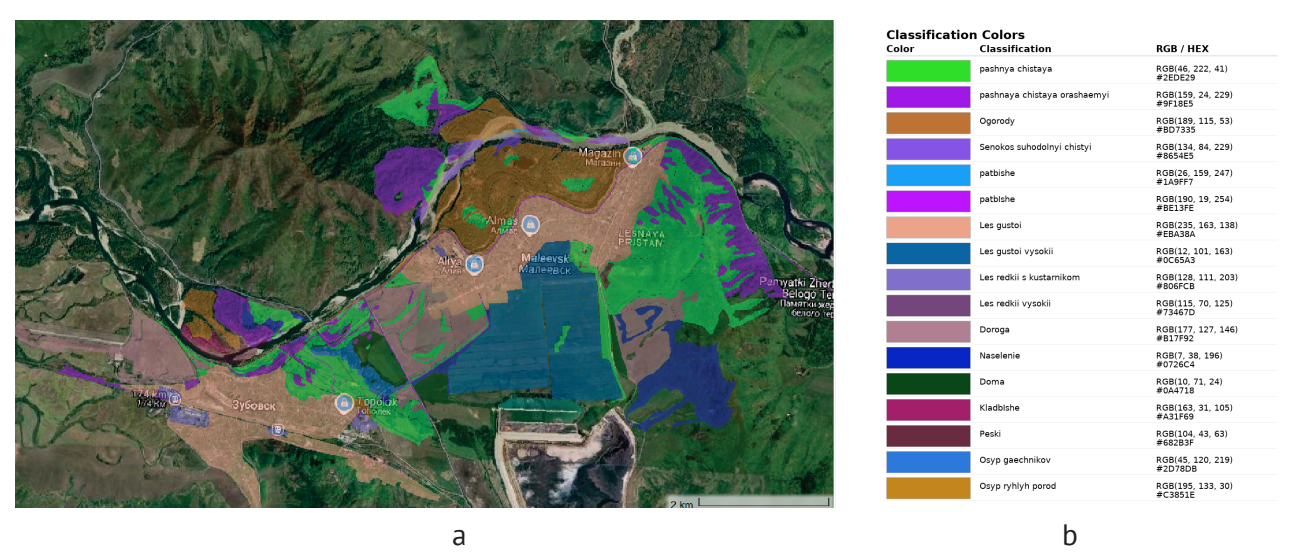


Figure 1. a) Custom HEC-RAS layer showing land-use polygons with assigned Manning's n-values.

B) A legend describing the colors and their affiliations

The two-dimensional computational area was developed with consideration of the site's morphological and landscape characteristics. Boundary conditions were defined using flow and stage hydrographs, and the hydraulic calculations were performed by solving the full momentum equations. The model used a uniform grid spacing of 5 m, with a 1-minute time step and 1-hour output interval. The computational area includes a 7.5 km section of the Buktyrma River within the village of Lesnaya Pristan.

Figure 2 shows the layout of the computational area used for one-dimensional (1D) modeling in HEC-RAS 6.6. The river centerline, along which cross sections are generated, is marked in green, while the cross sections themselves are shown in blue. These sections define the channel geometry required for performing hydraulic calculations. Station numbering is displayed in schematic meters, measured from the downstream boundary of the model upstream. The model covers a channel segment approximately 7.5 km long, between the hydrological station "Buktyrma – Lesnaya Pristan" and the upstream boundary of the computational area.

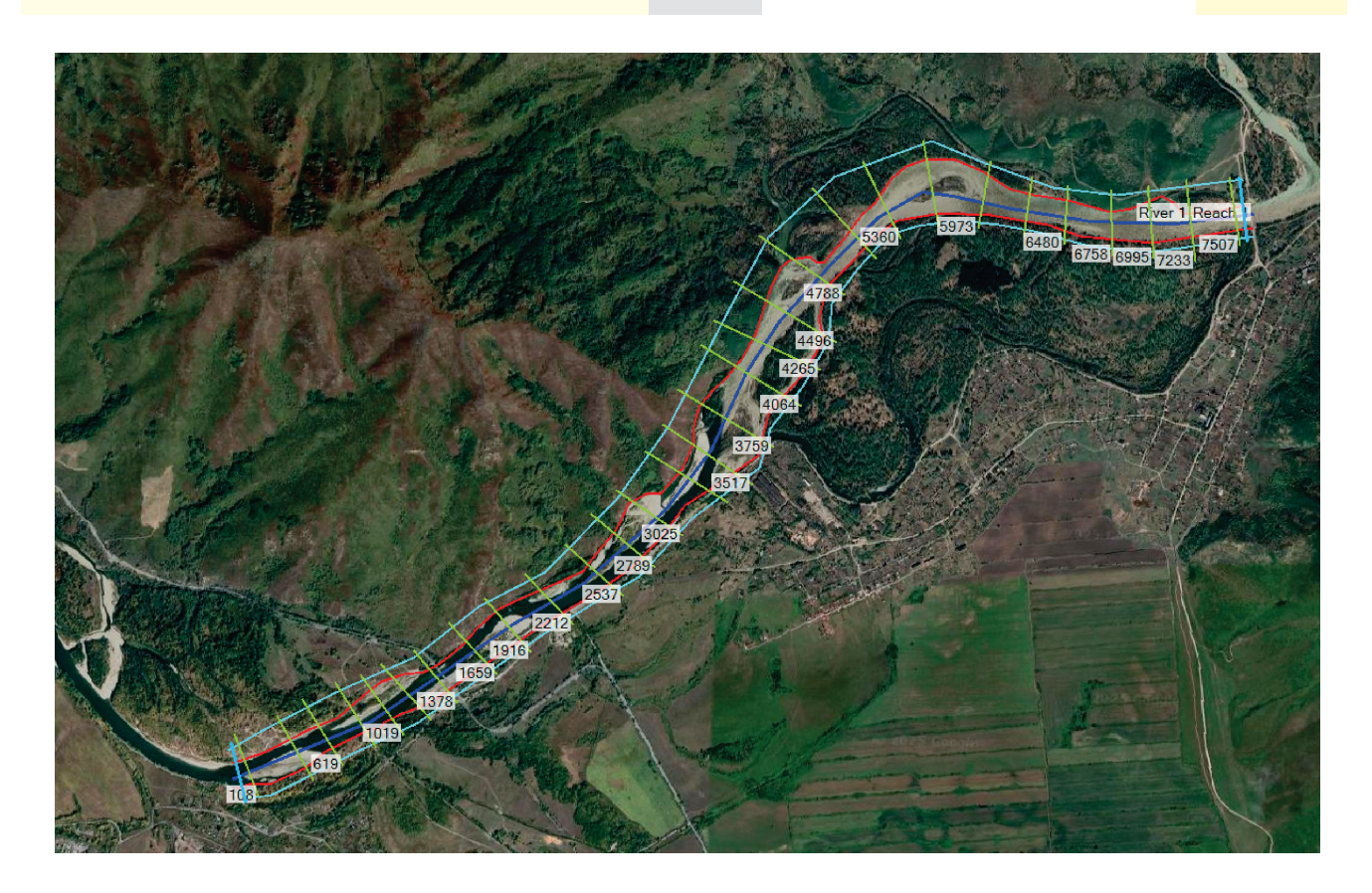


Figure 2. HEC-RAS 1D schematic with centerline (green) and cross-sections (blue), covering the 7.5 km model reach.

Model verification using satellite data

For the verification of the spatial distribution of flooding, remote sensing data were used. A multispectral Landsat 7 ETM+ image from April 1, 2018 (Tier 1) was selected for analysis. The image was acquired at a solar angle of 42° with 18% cloud cover.

Due to the scan line corrector (SLC) failure of Landsat 7 in May 2003, the image contains characteristic linear gaps (~390 m wide). These SLC-off stripes were corrected using masking and nearest-neighbor interpolation, which preserved the scene's suitability for hydrological analysis [23].

For the quantitative assessment of surface water saturation, the NDWI index was applied:

$$NDWI = \frac{G - NIR}{G + NIR},\tag{8}$$

where G is the reflectance value in the green band, and NIR is the reflectance value in the near-infrared band.

NDWI values make it possible to classify the Earth's surface according to the degree of water saturation. Positive values (0.2-1) indicate the presence of open water bodies such as rivers, lakes, and reservoirs. The range 0-0.2 corresponds to wet or temporarily flooded areas, including wetlands and agricultural lands. Negative values from -0.3 to 0 are typical of moderately dry areas with low-moisture vegetation, while values from -1 to -0.3 characterize dry, low-moisture zones with urbanized, rocky, or sandy landscapes.

Results

Validation of modeled flooding

The comparison between simulated flood area (HEC-RAS 6.6) and observed surface water derived from NDWI analysis revealed strong spatial agreement. The highest agreement is observed in the channel zone and floodplain areas, where modeled and satellite-derived in-undation boundaries closely aligned (Figure 3).

Agreement was also recorded in the settlements of Maleevsk and Zubovka. At the same time, local discrepancies were noted in the urban area of the city of Altai and along certain transportation corridors. In these zones, the NDWI map indicated a wider spread of surface moisture compared to the model. The most probable causes of such discrepancies are:

- accumulation of floodwaters in road embankments and ditches not captured at the current resolution of the digital elevation model;
- high vegetation moisture content generating a false-positive NDWI signal;
- artifacts from Landsat-7 sensor scan line corrector (SLC-off) failures, leading to partially incorrect representation of water bodies.

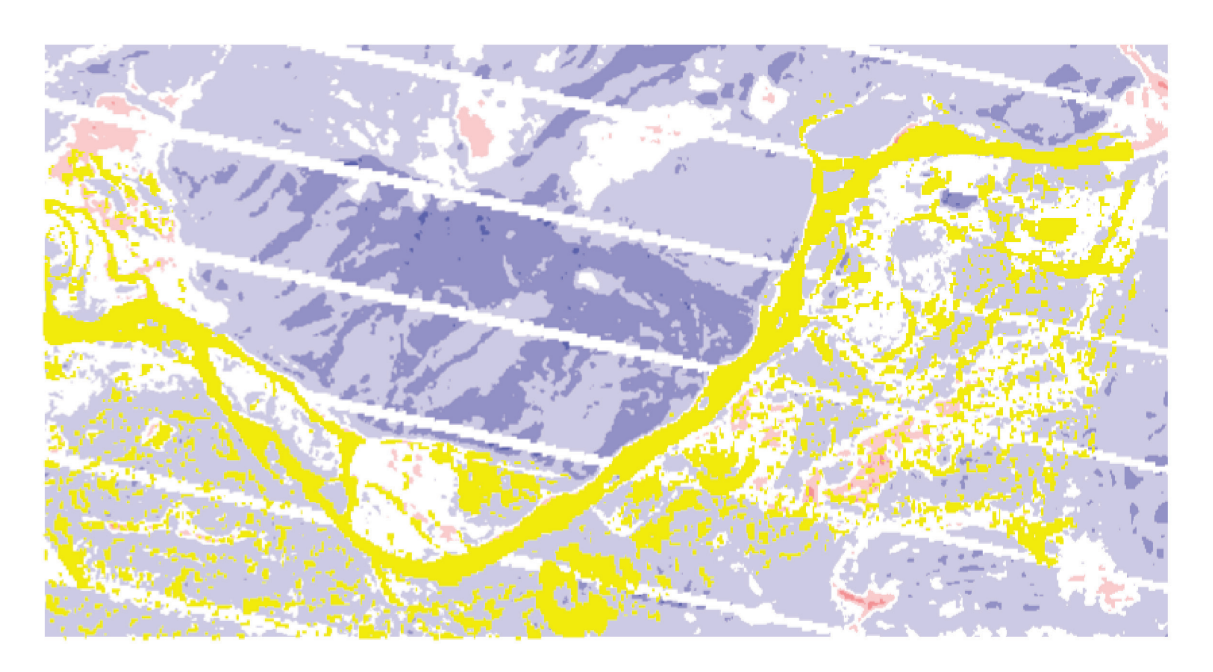


Figure 3. Overlay of the flood map (HEC-RAS, bright yellow outline) and the NDWI map on a satellite basemap in QGIS.

According to the NDWI classification, the total flood area amounted to 44.74 km^2 , of which 1.81 km^2 ($\approx 4\%$) correspond to cells with NDWI > 0.1, representing reliably flooded areas. This is in close agreement with the modeled inundation of 1.78 km^2 , with a difference of less than 1.6%, indicating high simulation accuracy.

The absence of NDWI values > 0.3 is explained by the lack of large, permanent water bodies in the scene and the predominance of fragmented or shallow inundation. Small positive areas within the -0.3 to -0.2 and 0.2 to 0.3 ranges are attributed to mixed pixels, especially along the edges of Landsat-7 SLC-off stripes. These do not significantly affect the overall flood area calculation (Figure 4).

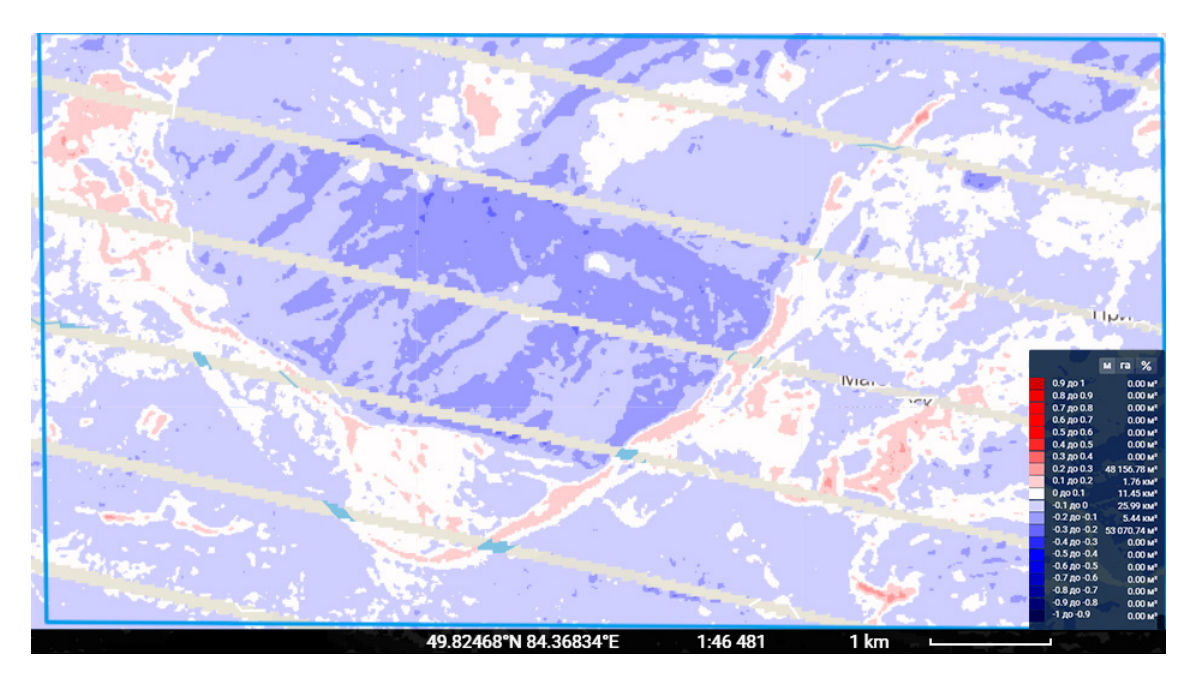


Figure 4. Spatial distribution of NDWI values in the Buktyrma River basin based on a Landsat-7 image from April 1, 2018.

Spatial dynamics of modeled flooding

The JRC Global Surface Water dataset was overlaid with settlement boundaries to compare historical water presence patterns with the 2018 event. The Global Surface Water – Occurrence layer reflects the probability of open water over a 38-year Landsat archive (1984–2022). Spatial agreement was observed between historically persistent wet zones and the modeled 2018 flood area (Figure 5).

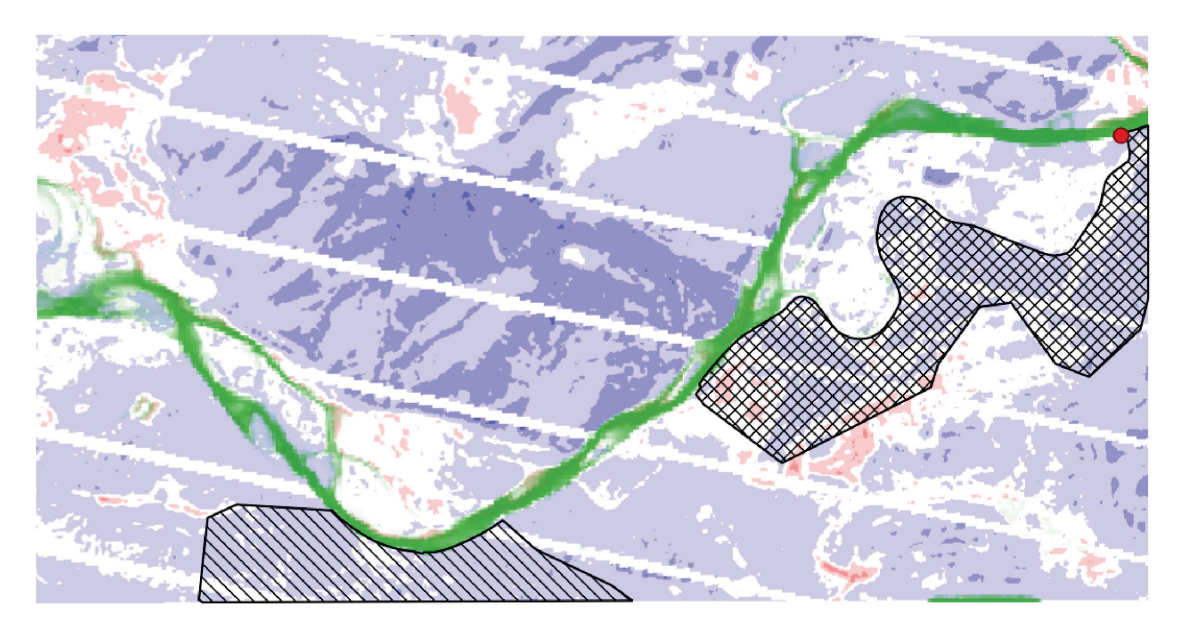


Figure 5. Integration of spatial layers: JRC Global Surface Water data (green), vector boundaries of Zubovka (hatching) and Maleevsk (grid), and the coordinates of the hydrological station "Buktyrma – Lesnaya Pristan" (red marker).

Figure 6 illustrates the spatial distribution of flow velocities in the river channel, based on one-dimensional hydraulic modeling results. The color scale shows velocity variation, from low values in stagnant or slow-moving zones to high values in channel constrictions and bends.

The model clearly identifies areas of potential bank erosion risk and highlights sections where flooding may occur with rising water levels. The discharge-weighted mean velocity along the 7 km modeled reach is approximately 1.1 m/s, with local values ranging between 0.3 and 2.0 m/s. These results reflect the typical hydraulic pattern of faster main-channel flow and slower velocities in floodplain sections.

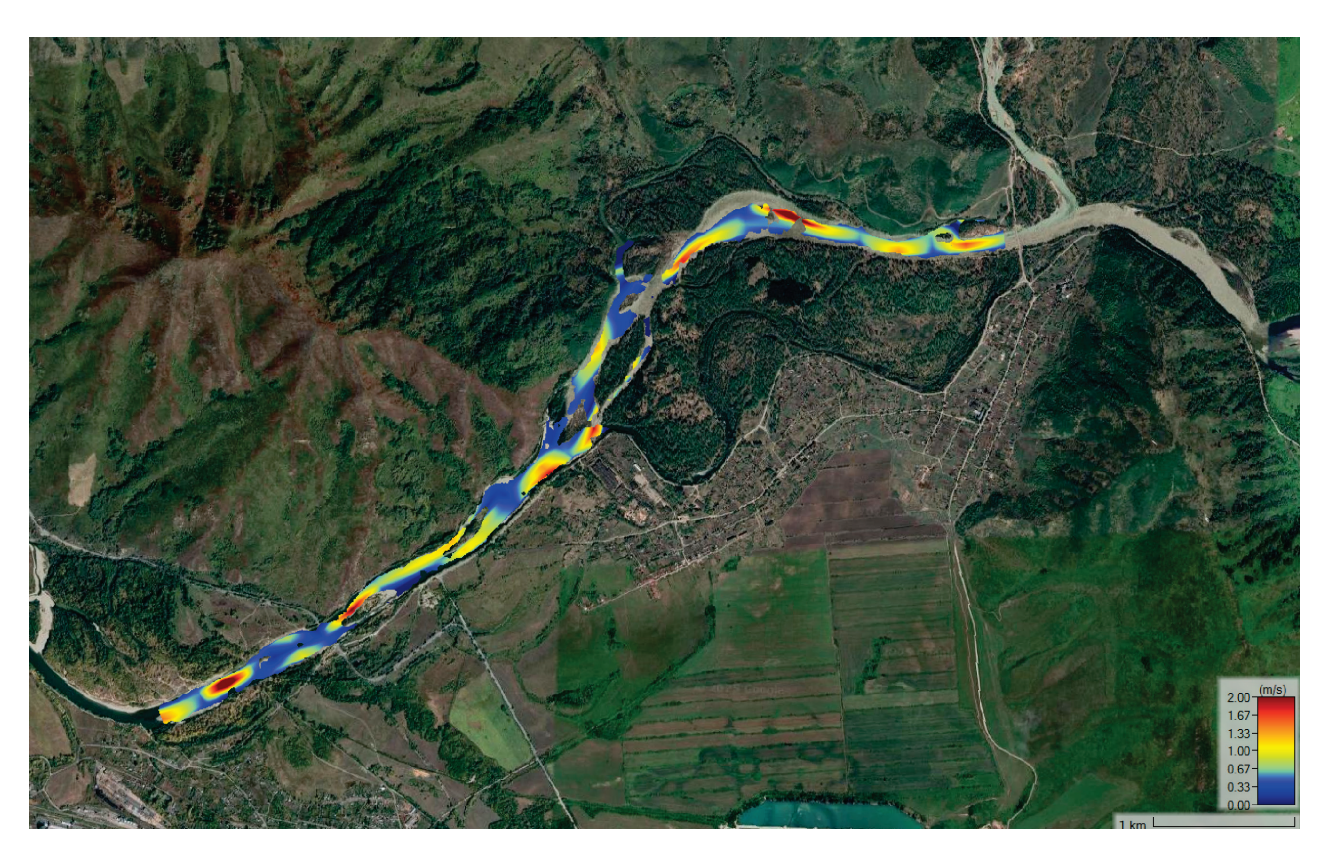


Figure 6. Distribution of flow velocities in the river channel based on the results of 1D hydraulic modeling in HEC-RAS.

Channel cross-sections and flood-depth profiles

Four representative cross-sections were extracted from the HEC-RAS geometry and adjusted using field observations (Figure 7). Channel widths ranged from 120 to 160 m, and depths from 1.8 to 3.5 m, reflecting the morphological variability along the valley (Table 3).

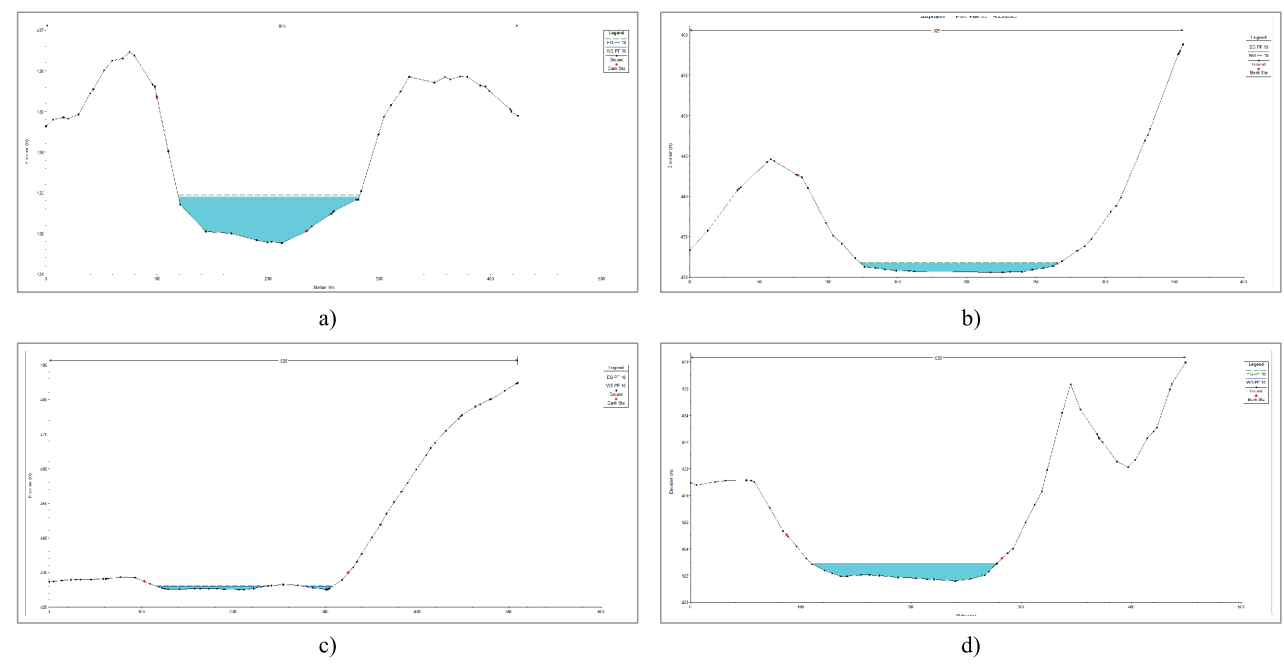


Figure 7. Cross-sectional profile of the river channel with water level shown in HEC-RAS, corresponding to selected computational cross sections of the model: a) 2507 m; b) 6480 m; c) 2789 m; d) 619 m.

Table 3 presents the key geometric parameters of cross sections of the Buktyrma River channel, automatically generated in HEC-RAS and adjusted based on field observations. As can be seen, the channel width varies from 120 to 160 meters, and the depth from 1.8 to 3.5 meters, reflecting both the morphological diversity of the valley and differences in hydraulic resistance and bank configuration along different segments.

Table 3. Geometric parameters of computational cross sections of the Buktyrma River channel according to HEC-RAS data.

Station (m)	Water surface width (m)	Maximum depth (m)
2507 м	approximately 120 m	approximately 3.5 m
6480 м (left floodplain area dry)	approximately 160 m	approximately 2.0 m
2789 м	approximately 140 m	approximately 1.8 m
619 м	approximately 130 m	approximately 3.0 m

The elevation comparison shows that at a water level of 425.74 m, the flow remains within the channel. Once the threshold of approximately 428.5 m is exceeded, overbank flow occurs, inundating near to agricultural and residential areas. Figure 8 illustrates potential water pathways and accumulation zones under further level increases.

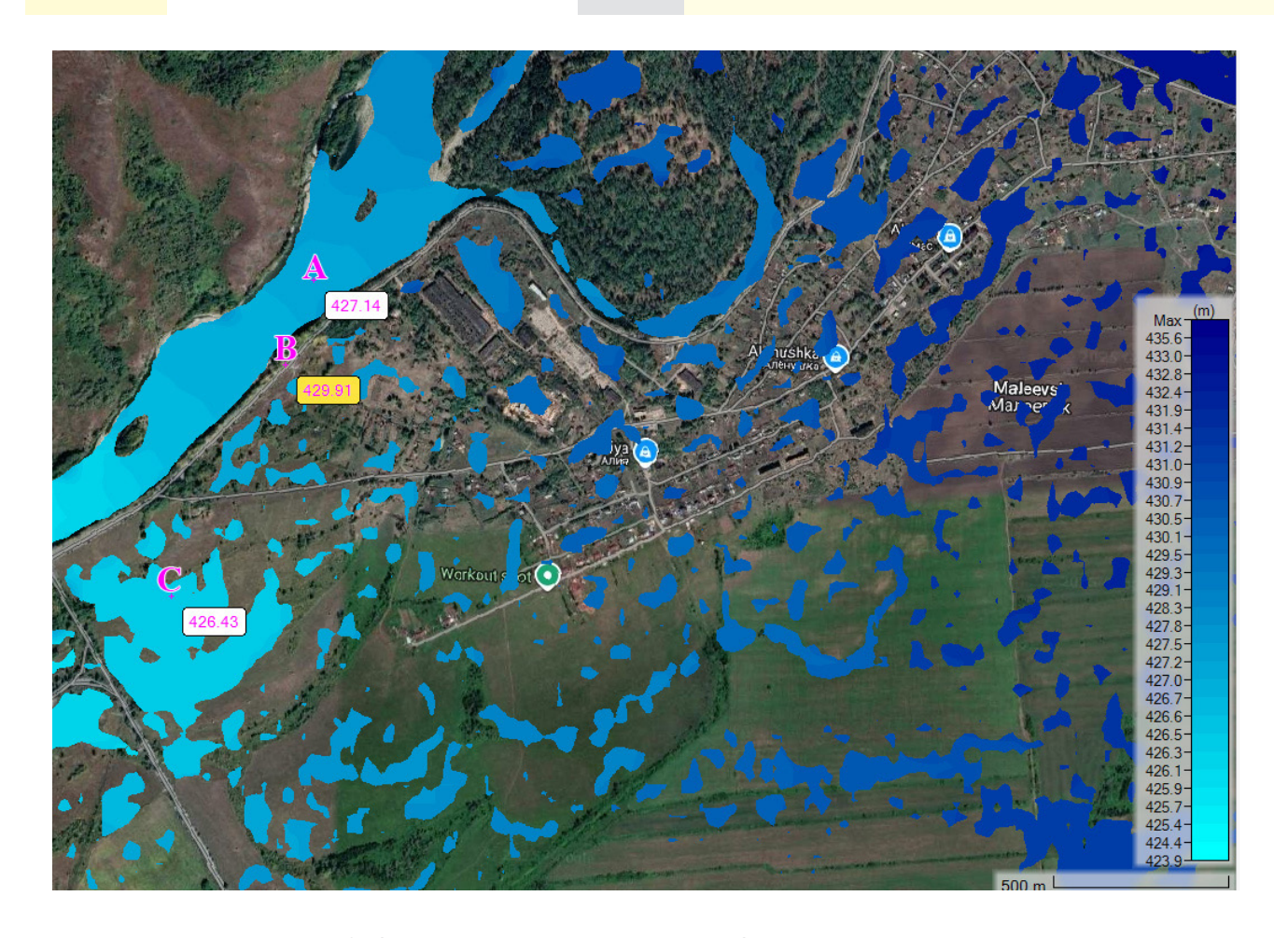


Figure 8. Cartographic representation of flood situation elements:

(A) water surface level in the river channel — 427.14 m (excluding water level, approx. 1.5 m);

(B) bank elevation — 429.91 m; (C) floodwater accumulation zone — 426.43 m

(excluding water level, approx. 0.3 m).

Final flood simulation map and web-GIS platform

The final flood-depth map (Figure 9) shows a strong spatial match with the officially recorded flood of 31 March 2018. Most flooded cells lie along the main channel of the Buktyrma River and its meandering branches, corresponding to orographically low-lying zones.

Water depth is represented using a blue gradient: light blue indicates shallow flooding, while darker shades denote deeper inundation. Areas of overbank flow are clearly visible, along with floodplain zones subject to partial or complete inundation.

Flood depths are visualized using a blue color gradient, from light (shallow) to dark (deep), clearly highlighting areas of overbank flow and floodplain inundation. Fragmented flood patches are visible, particularly on the left bank where quarries and other artificial excavations are located. On the right bank, localized flooding is associated with floodplain terraces and zones of woody-shrub vegetation, where high surface roughness slows the flow and promotes water accumulation.

Water accumulation zones were also recorded along transport infrastructure, indicating the role of road embankments as hydraulic barriers influencing the redistribution of flood flows. A comparison with the cadastral map shows that the flooded agricultural land in this section accounts for about 42% of the total flood perimeter, whereas the share of built-up areas does not exceed 6%.



Figure 9. Flood map based on HEC-RAS 6.6 modeling results. Blue shades correspond to different flood depths.

An interactive flood map was also developed using model outputs and integrated into a custom web-GIS platform (Figure 10). The interface allows users to explore flood contours in real time, zoom to areas of interest, switch data layers, and access attribute information for selected objects.

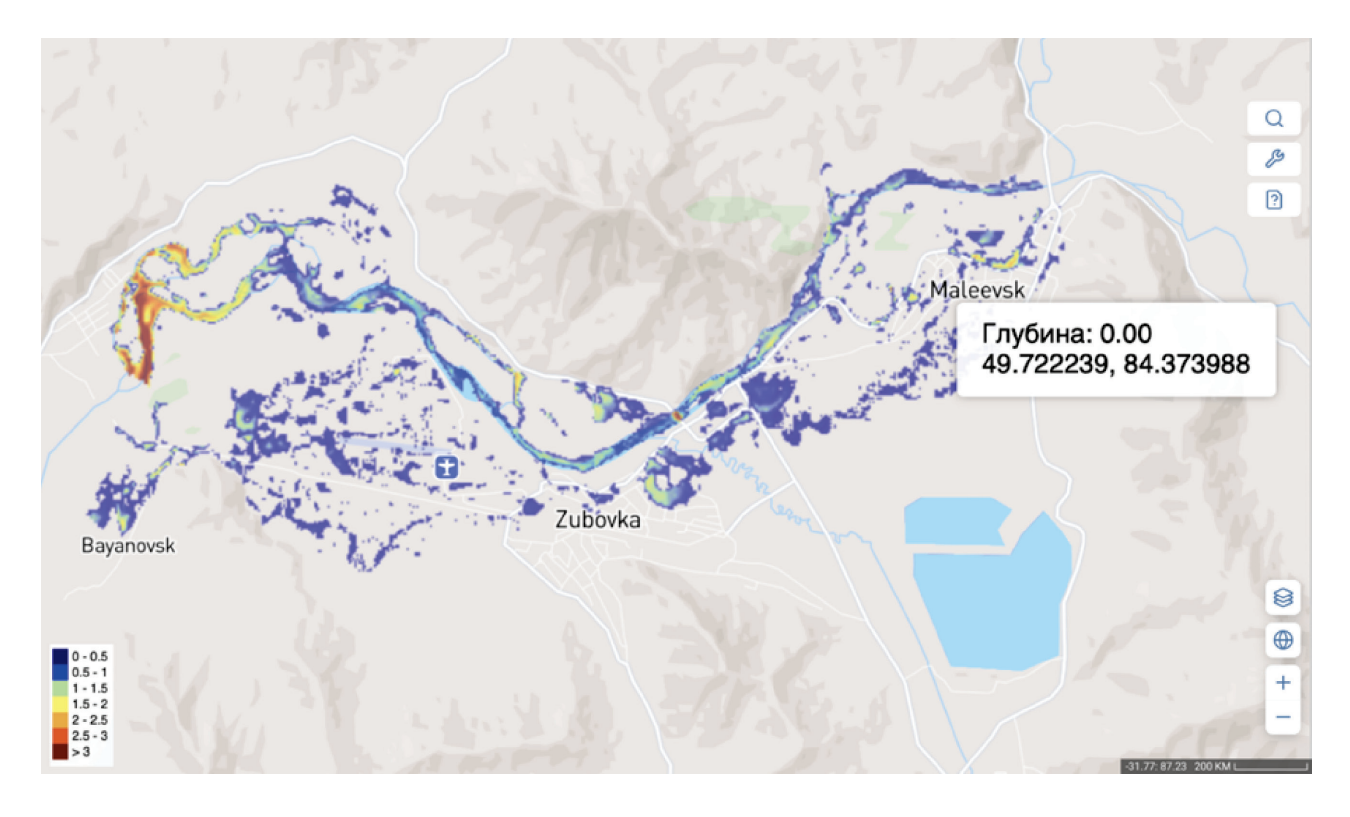


Figure 10. Visualization of modeling results in the Web-GIS platform.

The platform is intended to improve public and institutional access to flood risk information and to support decision-making at the municipal and regional levels.

Discussion

The comparison of 2D modeling results in HEC-RAS with the flood map derived from the NDWI index revealed local discrepancies in the shape and area of floodwater. These are attributed both to the exceptional hydrometeorological conditions of spring 2018 and to inherent limitations of the numerical scheme. Experts from the Altai District local administration explained that the extreme flood was the result of a combination of rare factors:

- a low snow but very cold winter (snow covers up to 105 cm, ground freezing to 1.5 m, river ice thickness up to 2 m);
- a sharp warming on March 31 accompanied by heavy rainfall;
- avalanche-like snowmelt and the formation of ice jams, which led to exceedance of critical levels on the Buktyrma River (7.10 m versus a critical level of 5.30 m) and the Berezovka River (4.0 m versus a critical level of 2.0 m).

These processes caused flooding in Altai (formerly Zyryanovsk) and nearby villages, resulting in the declaration of a state of emergency.

The model did not account for spatially distributed snowmelt, inflows from frozen slopes, ice jam dynamics, local overflows across eroded banks, or the microrelief of the floodplain. The fixed grid with a 30 m resolution smoothed small depressions where NDWI detected isolated inundation. Taken together, this explains the local discrepancies: satellite data indicate somewhat more extensive flooded areas along roads and in lowlands than the computational scheme. Nevertheless, the total inundation area calculated by the model (1.78 km²) differs from the satellite-based estimate by only 1.6%, while contour overlap using the intersection method reaches 87%. To further improve accuracy, it would be advisable to couple HEC-RAS with a snowmelt-runoff module (e.g., HEC-HMS), apply a more detailed adaptive grid, incorporate ice-jam scenarios, and calibrate the results using a series of high-resolution images (Sentinel-1/2, PlanetScope). Thus, the observed discrepancies represent an explainable difference between an idealized hydrodynamic simulation and the actual emergency and do not diminish the overall reliability of the model for forecasting and planning tasks.

Overall, the agreement between simulated and satellite-derived flood areas confirms that reliable flood mapping can be achieved with open hydrological and topographic data. The results align with earlier studies that report high HEC-RAS accuracy for local-scale modeling under limited-data conditions [19]. Nevertheless, the identified discrepancies – such as the underestimation of flooding along roads and in depressions – highlight the need to account for additional factors, including microrelief, snow cover, ice jams, and urban infrastructure.

Conclusion

This study demonstrates the effectiveness of a reproducible, data-efficient approach for two-dimensional flood modeling and spatial visualisation, using the 2018 flood event in the Buktyrma River basin as a representative case. The work relied exclusively freely available data and tools, including HEC-RAS 6.6 software package, the Copernicus 30m DEM, satellite-derived NDWI indices (Landsat-7), and land-cover-based Manning's roughness coefficients.

The model demonstrated high agreement with observed flood areas (the calculated flood area differed from satellite-derived estimates by less than 2%, and the contour overlap reached 87%). This confirms the reliability of the approach and its applicability under conditions of limited access to detailed hydrological information.

Given its scalability, transparency, and low cost, the proposed methodology is well suited for deployment in other flood-prone regions of Kazakhstan. It holds practical value for spatial

© Nurassyl Zhomartkan, Anatoliy Pavlenko, Yerzhan Baiburin, Mohammad Alhuyi-Nazari

planning, flood risk assessment, the design of protective infrastructure, and the development of early warning systems.

Acknowledgment

This work has been funded by the Science Committee of the Ministry of Science and Higher Education of the Republic of Kazakhstan (Grant Number BR24992899) within the framework of the project «Development of a system for forecasting catastrophic floods in the East Kazakhstan region using remote sensing data, GIS technologies, and machine learning».

References

- [1] Chan, S. W., Abid, S. K., Sulaiman, N., Nazir, U., & Azam, K. (2022). A systematic review of the flood vulnerability using geographic information system, Heliyon 8 (3), 1-11. https://doi.org/10.1016/j. heliyon.2022.e09075
- [2] Ngenyam Bang, H., & Church Burton, N. (2021). Contemporary flood risk perceptions in England: Implications for flood risk management foresight. Climate Risk Management, 32, 100317. https://doi.org/10.1016/j.crm.2021.100317
- [3] Chettykbayev, R. K., & Denisova, N. F. (2020). Analysis of computer modeling tools for assessing the risk of flooding in the East Kazakhstan region. In Digitalization and Industry 4.0: Economic and Societal Development: An International and Interdisciplinary Exchange of Views and Ideas (pp. 283-290). Wiesbaden: Springer Fachmedien Wiesbaden. https://doi.org/10.1007/978-3-658-27110-7 20
- [4] Mihu-Pintilie, A., Cîmpianu, C. I., Stoleriu, C. C., Pérez, M. N., & Paveluc, L. E. (2019). Using high-density LiDAR data and 2D streamflow hydraulic modeling to improve urban flood hazard maps: A HEC-RAS multi-scenario approach. Water, 11(9), 1832. https://doi.org/10.3390/w11091832
- [5] Shustikova, I., Domeneghetti, A., Neal, J. C., Bates, P., & Castellarin, A. (2019). Comparing 2D capabilities of HEC-RAS and LISFLOOD-FP on complex topography. Hydrological Sciences Journal, 64(14), 1769–1782. https://doi.org/10.1080/02626667.2019.1671982
- [6] Djafri, S. A., Cherhabil, S., Hafnaoui, M. A., & Madi, M. (2024). Flood modeling using HEC-RAS 2D and IBER 2D: A comparative study. Water Supply, 24(9), 3061–3076. https://doi.org/10.2166/ws.2024.184
- [7] Lidberg, W., Nilsson, M., Lundmark, T., & Ågren, A. M. (2017). Evaluating preprocessing methods of digital elevation models for hydrological modelling. Hydrological Processes, 31(26), 4660–4668. https://doi.org/10.1002/hyp.11385
- [8] Ansarifard, S., et al. (2024). Simulation of floods under the influence of effective factors in hydraulic and hydrological models using HEC-RAS and MIKE 21. Discover Water, 4(1), 92. https://doi.org/10.1007/s43832-024-00155-0
- [9] Tamiru, H., & Dinka, M. O. (2021). Application of ANN and HEC-RAS model for flood inundation mapping in lower Baro Akobo River Basin, Ethiopia. Journal of Hydrology: Regional Studies, 36, 100855. https://doi.org/10.1016/j.ejrh.2021.100855
- [10] Brunner, G. (2018). Benchmarking of the HEC-RAS two-dimensional hydraulic modeling capabilities. US Army Corps of Engineers: Davis, CA, USA, 1-137. https://www.hec.usace.army.mil/software/hec-ras/documentation/RD-51_Benchmarking_2D.pdf
- [11] Ongdas, N., Akiyanova, F., Karakulov, Y., Muratbayeva, A., & Zinabdin, N. (2020). Application of HEC-RAS (2D) for flood hazard maps generation for Yesil (Ishim) River in Kazakhstan. Water, 12(10), 2672. https://doi.org/10.3390/w12102672
- [12] Kalashnikova, O., Nurbacina, A., & Niyazov, D. (2023). Otsenka riskov navodnenii i pavodkov v tselyakh ustoichivogo razvitiya v basseine reki Zhabai (Kazakhstan) [Assessment of flood and high-water risks for sustainable development in the Zhabai River basin (Kazakhstan)]. Central Asian Journal of Water Research, 2(1), 22–45. https://doi.org/10.29258/CAJSCR/2023-R1.v2-1/22-45.rus
- [13] Akiyanova, F., et al. (2023). Operation of gate-controlled irrigation system using HEC-RAS 2D for spring flood hazard reduction. Computation, 11(2), 27. https://doi.org/10.3390/computation11020027

- [14] Kumar, V., Sharma, K., Caloiero, T., Mehta, D., & Singh, K. (2023). Comprehensive overview of flood modeling approaches: A review of recent advances. Hydrology, 10(7), 141. https://doi.org/10.3390/ hydrology10070141
- [15] Costabile, P., Costanzo, C., Ferraro, D., Macchione, F., & Petaccia, G. (2020). Performances of the new HEC-RAS version 5 for 2-D hydrodynamic-based rainfall-runoff simulations at basin scale: Comparison with a state-of-the-art model. Water, 12(9), 2326. https://doi.org/10.3390/w12092326
- [16] Liu, Z., Merwade, V., & Jafarzadegan, K. (2019). Investigating the role of model structure and surface roughness in generating flood inundation extents using one- and two-dimensional hydraulic models. Journal of Flood Risk Management, 12(1), e12347. https://doi.org/10.1111/jfr3.12347
- [17] Kim, B., Sanders, B. F., Schubert, J. E., & Famiglietti, J. S. (2014). Mesh type tradeoffs in 2D hydrodynamic modeling of flood inundation. Advances in Water Resources, 68, 42–61. https://doi.org/10.1016/j.advwatres.2014.02.013
- [18] Sikan, A. V. (2020). Veroiatnostnye raspredeleniia v gidrologii [Probability distributions in hydrology], 286. http://elib.rshu.ru/files_books/pdf/rid_87d638c890a947f99fcec9099b397e64.pdf
- [19] European Space Agency (2024). Copernicus Global Digital Elevation Model. Distributed by Open-Topography. https://doi.org/10.5069/G9028PQB. Accessed 2025-04-04
- [20] McFeeters, S. K. (1996). The use of the normalized difference water index (NDWI) in the delineation of open water features. International Journal of Remote Sensing, 17(7), 1425–1432. https://doi.org/10.1080/01431169608948714
- [21] Komitet po upravleniiu zemel'nymi resursami Ministerstva sel'skogo khoziaistva Respubliki Kazakhstan. (2025, April 15). Publichnaia kadastrivaia karta Respubliki Kazakhstan [Public cadastral map of the Republic of Kazakhstan]. https://map.gov4c.kz/egkn/
- [22] Dorin, G. et al. (2022). Mathematical modelling and numerical analysis of hydraulic system behaviour: A case study with application in HEC-RAS. IOP Conference Series: Materials Science and Engineering, 1256(1), 012027. IOP Publishing. https://doi.org/10.1088/1757-899X/1256/1/012027
- [23] Hossain, M. S., Bujang, J. S., Zakaria, M. H., & Hashim, M. (2015). Assessment of Landsat 7 Scan Line Corrector-off data gap-filling methods for seagrass distribution mapping. International Journal of Remote Sensing, 36(4), 1188–1215. https://doi.org/10.1080/01431161.2015.1007257